

# Energy Spectrum of Spin Fluctuations in Superconducting $\text{La}_{2-x}\text{Sr}_x\text{CuO}_4$

( $0.10 \leq x \leq 0.25$ )

Chul-Ho Lee\*, Kazuyoshi Yamada†, Yasuo Endoh

*Department of Physics, Tohoku University, Aramaki Aoba, Sendai 980-77, Japan*

Gen Shirane

*Department of Physics, Brookhaven National Laboratory, Upton, NY 11973-5000, USA*

R. J. Birgeneau, M. A. Kastner, M. Greven‡, Y-J. Kim

*Department of Physics and Center for Materials Science and Engineering, Massachusetts Institute of Technology, Cambridge, MA 02139, USA*

November 12, 1999

The energy spectrum of incommensurate spin fluctuations in superconducting Sr-doped  $\text{La}_2\text{CuO}_4$  has been studied by inelastic neutron scattering experiments. An energy gap in the spin excitation spectrum is observed in the superconducting state of optimally doped ( $x=0.15$ ) and slightly overdoped ( $x=0.18$ ) samples. At temperatures well below  $T_c$ , the incommensurate peaks diminish rapidly in intensity with decreasing energy below  $\sim 8\text{meV}$  and merge into the background below  $\sim 3.5\text{meV}$  for  $x=0.15$  and  $\sim 4.5\text{meV}$  for  $x=0.18$ . For both samples, the energy spectrum of the  $q$ -integrated spin susceptibility,  $\chi''(\omega)$ , exhibits an enhancement around  $7\text{meV}$ , which is caused by a broadening in the momentum width of the incommensurate peaks. The gap-like structure in the energy spectrum and the enhancement of  $\chi''(\omega)$  survive at  $T_c$ . On the other hand, for both underdoped ( $x=0.10$ ) and heavily overdoped ( $x=0.25$ ) samples there is neither a clear energy gap nor an enhancement of  $\chi''(\omega)$  below  $T_c$ .

KEYWORDS:  $\text{La}_{2-x}\text{Sr}_x\text{CuO}_4$ , high- $T_c$  superconductor, spin fluctuation, neutron scattering

## I. Introduction

The interplay between magnetism and superconductivity is one of the most interesting and important issues in the physics of the cuprate high temperature superconductors [1]. For more than ten years, experimental studies on the spin fluctuations in these materials have been performed by neutron scattering and NMR measurements. NMR first revealed

a suppression of the low-energy spin excitations below what is called the spin gap temperature [2]. In the underdoped region, it is thought that above  $T_c$  a pseudo-gap opens up in the spin fluctuation spectrum. Since the spin-gap state is believed to be related to the pairing mechanism, a large number of experimental and theoretical studies have focused on the origin of the spin gap.

Unlike NMR, neutron scattering can determine both the momentum and the energy dependence of the magnetic excitations, providing information about the anisotropy of the energy gap of the high- $T_c$  cuprates. In fact, neutron scattering has been used to observe the spin-gap of  $\text{YBa}_2\text{Cu}_3\text{O}_{7-y}$  by

\* Permanent address: Electrotechnical Laboratory, Umezono 1-1-4 Tsukuba, 305-8568, Japan

† Permanent address: Institute for Chemical Research, Kyoto University, Uji 611-0011, Japan

‡ Permanent address: Dept. of Applied Physics, Stanford University, Stanford, CA 94305, USA

determining the energy spectrum of the dynamical spin susceptibility  $\chi''(q, \omega)$  around  $(\pi, \pi)$  as a function of  $T$  [3,4,5]. However, the energy spectrum of the spin fluctuations and its doping dependence in  $\text{La}_{2-x}\text{Sr}_x\text{CuO}_4$  have not yet been determined over a wide range of  $x$ , most especially for  $x$  above the optimal doping value. This is in part because it is difficult to separate the weak magnetic signals from the non-magnetic background originating from phonons for example. Further, it is difficult to grow large homogeneous single crystals over a wide doping region.

Several years ago an overview of the low energy spectrum of  $\chi''(q, \omega)$  associated with the incommensurate peaks of  $\text{La}_{1.85}\text{Sr}_{0.15}\text{CuO}_4$  was presented [6]. Shortly thereafter, a well-defined energy gap of  $\gtrsim 3.5\text{meV}$  was observed in the superconducting state of the optimally Sr-doped  $\text{La}_2\text{CuO}_4$  [7]. The latter measurements were limited to low energies  $\lesssim 6\text{meV}$ . For higher energies, pulsed neutron scattering measurements were performed on  $\text{La}_{1.85}\text{Sr}_{0.15}\text{CuO}_4$  and revealed a broad peak between  $\omega = 40$  and  $70\text{meV}$  [8] in  $\chi''(\omega)$ . The dynamical spin susceptibility was integrated over  $q$  around the incommensurate peaks. This result was recently reconfirmed by more comprehensive experiments and analysis on the same crystals [9].

However, Hayden *et al.* [10] reported a somewhat sharper peak in the energy spectrum of  $\chi''(\omega)$  at around  $\omega = 20\text{meV}$  in  $\text{La}_{1.86}\text{Sr}_{0.14}\text{CuO}_4$  by combining data taken by pulsed neutron scattering with that of 3-axis neutron spectroscopy. Furthermore, the latter group studied the energy and temperature dependence of  $\chi''(\omega)$  using the same crystal and suggested that they were observing the effects of a nearby quantum critical point at  $T=0\text{ K}$ . They reported that the  $q$ -width of the spin fluctuations monotonically increased with increases in either temperature or energy [11] although their observed cor-

relation length at low temperatures was in fact quite short in apparent contradiction with the quantum critical interpretation. They found no evidence for a gap in the spin fluctuation spectrum above  $T_c$ , in conflict with NMR measurements [12].

To reconcile these apparent inconsistencies a more systematic neutron scattering study is required. In particular, it is important to measure the doping dependence of the energy spectrum over a wide doping region. To accomplish this we have grown large single crystals of superconducting Sr-doped  $\text{La}_2\text{CuO}_4$  over a wide range of Sr concentrations extending from the underdoped to the highly overdoped region. Although the energy region in the present study is still limited to that of conventional low energy 3-axis neutron scattering measurements, the doping dependence provides new insights into the spectrum of the spin fluctuations in this system. We describe the experimental details in section II, the results and data analysis are presented in section III, a discussion is given in section IV and a brief summary is presented in section V.

## II. Experimental Detail

Single crystals of  $\text{La}_{2-x}\text{Sr}_x\text{CuO}_4$  have been grown by the traveling solvent floating zone (TSFZ) method using lamp-image furnaces [13,14]. The furnaces have been improved in order to tune the temperature gradient near the molten zone. We have found that a steep temperature gradient around the liquid allows us to grow homogeneous large single crystals. As-grown single crystals have been kept under oxygen flow at  $900^\circ\text{C}$  for 50 hours to remove oxygen defects.

To characterize the Sr content and homogeneity we determined the phase transition temperature ( $T_s$ ) between the high temperature tetragonal (HTT) and the low temperature orthorhombic

(LTO) phases by neutron diffraction. The values for  $T_s$  of our single crystals [15] agree quite well with those previously deduced from powder data [16,17,18].  $T_s$  depends primarily on the Sr concentration and specifically a small amount of oxygen non-stoichiometry does not change  $T_s$  appreciably [19,20]. Therefore, the agreement of the measured  $T_s$  for our single crystals with the results obtained from measurements on powders confirms the Sr concentration of our single crystals. The values of the Sr concentration measured by electron probe micro-analysis were also consistent with the results from the  $T_s$  measurements within the instrumental resolution.

Superconducting magnetic shielding effects were measured by a SQUID magnetometer in a magnetic field of 10 Oe. The onset temperature of the superconducting transition ( $T_c$ ) in the  $x = 0.15$  single crystal,  $T_c = 37.5$ K, is almost the same as the maximum value found in powder samples [18,21]. For  $x = 0.10, 0.18$  and  $0.25$  the values of  $T_c = 29$ K, 36.5K and 15K, respectively, also agree with those of powder samples [15]. Since  $T_c$  is very sensitive to any deviation from stoichiometry in the oxygen concentration [20,22], this agreement suggests that the oxygen content and ordering of our crystals is nearly optimal.

Normal state magnetic susceptibilities were also measured using a SQUID magnetometer with a magnetic field of 1T. We observed a broad peak at a temperature  $T_{max} = 200$ K for  $x = 0.18$  which depends on both the Sr and the oxygen concentration [22].  $T_{max}$  of the single crystal is in good agreement with that of a powder sample with the same Sr concentration [22, 23, 24]. Lattice parameters of pulverized single crystals measured by x-ray diffraction at room temperature are also consistent with previous data [15].

Inelastic neutron scattering measurements were performed with the triple-axis spectrometer, TOPAN at JRR-3M in the Tokai Establishment of JAERI for crystals with  $x = 0.15, 0.18$ , and  $0.25$  and with H7 at the HFBR at Brookhaven National Laboratory for crystals with  $x = 0.10$  and  $0.15$ . The incident (final) neutron energy was typically fixed at  $E_i$  ( $E_f$ ) = 14.75meV for TOPAN and  $E_i$  ( $E_f$ ) = 14.7meV for H7. A typical sequence of the horizontal collimators was 40'-100'-S-60'-B for TOPAN and 40'-40'-S-80'-80' for H7 where S denotes the sample position. Pyrolytic graphite crystals were used both as monochromator and analyzer. A pyrolytic graphite filter was used to reduce the intensity of higher order neutrons. Moreover, in TOPAN, a sapphire crystal was inserted to reduce significantly the flux of high energy neutrons. The single crystals were mounted in an Al container filled with He gas as a heat exchanger. For cooling, a closed cycle He refrigerator was used.

### III. Results

The four panels in Fig. 1 show representative  $q$ -spectra of the magnetic fluctuations measured at and below  $T_c$ . Constant-energy scans were performed through the two peaks at  $(\pi, \pi(1 \pm \delta))$  as illustrated in the inset of panel (c). For  $x = 0.18$ , due to some non-magnetic contamination in the scan, we present only one of the peaks, at  $(\pi, \pi(1 - \delta))$ . For  $T \gtrsim T_c$  well-defined peaks are observed at incommensurate positions for all samples. Below  $T_c$ , the peaks at 3 meV and 3.5 meV vanish into the background for  $x = 0.15$  and  $0.18$  respectively. As is shown by the energy spectra discussed below, this dramatic change occurs due to the opening of an energy gap in the spin excitation spectrum at the same temperature as that for the onset of superconductivity. In contrast, for  $x = 0.10$  and  $0.25$  substantial peak

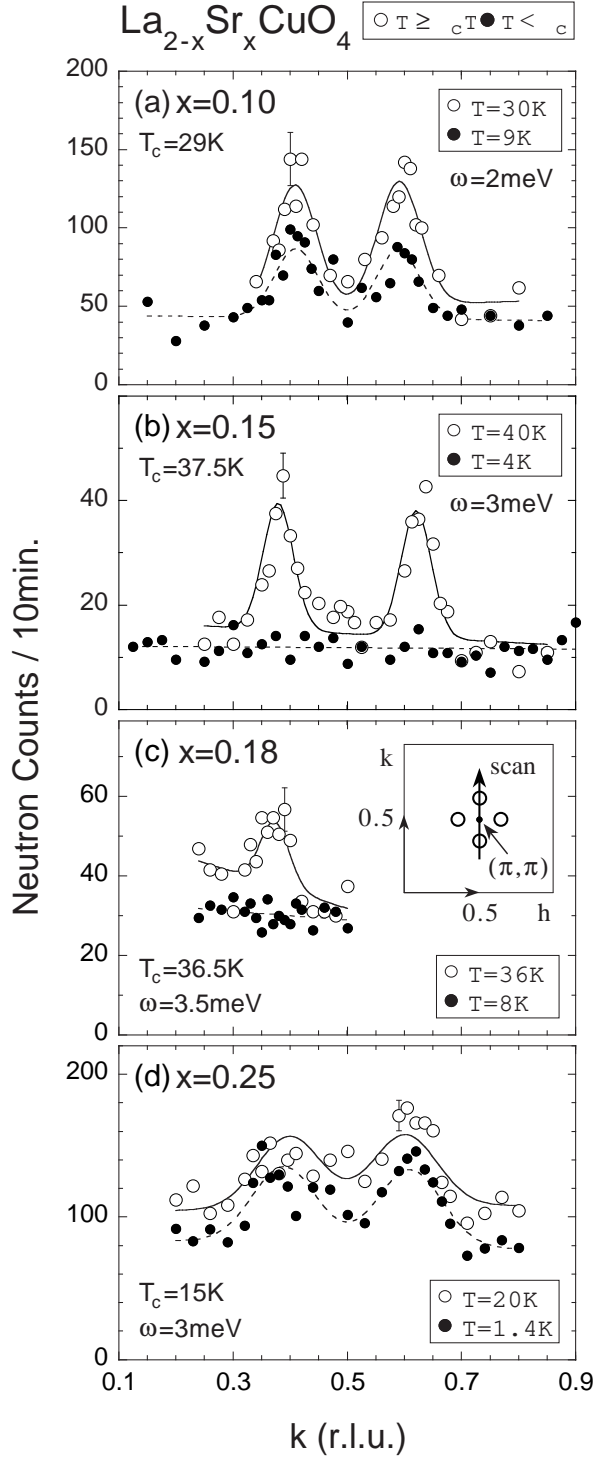


FIG. 1. Constant energy-scan across  $(\pi, \pi)$  as indicated in the inset of panel (c) for samples with (a)  $x=0.10$  (b)  $x=0.15$  (c)  $x=0.18$  and (d)  $x=0.25$  below and at  $T_c$ . All solid lines and dashed lines for  $x = 0.10$  and  $0.25$  are the results of least square fits to the data points using two Lorentzian functions convoluted with the instrumental resolution.

intensities at low energies are observed even at temperatures well below  $T_c$

We present the results of the same  $q$ -scan as that shown in Fig. 1 at several different energies for  $x=0.10$  and  $0.15$  in Figs. 2 and 3 respectively. Below  $T_c$ , the peak intensities for  $x=0.10$  are comparable at all energies between 2 and 10 meV. On the other hand, for  $x=0.15$  the intensities dramatically decrease with decreasing energy and no peak remains outside of the errors at 3 meV. Although our collaboration has reported the observation of an energy gap for  $x=0.15$  previously [7] the change in peak intensities below  $\sim 7$  meV appears to be more dramatic in these experiments. A similar energy dependence of the incommensurate peak intensity is found for  $x=0.18$  as shown in Fig. 4(c).

The  $q$ -spectrum of the incommensurate peaks was fitted using the following dynamical structure factor  $S(q, \omega)$  convoluted with the instrumental resolution function:

$$S(q, \omega) = \frac{I}{1 - \exp(-\frac{\omega}{\kappa_B T})} \cdot \chi''(q, \omega) \quad (1)$$

with

$$\chi''(q, \omega) = A_\omega \sum_{\delta=1,4} \left\{ \frac{\kappa_\omega}{|q - q_\delta|^2 + \kappa_\omega^2} \right\} \quad (2)$$

where  $q_g$ ,  $\kappa_\omega$ ,  $k_B$  and  $A_\omega$  are the peak positions of the magnetic peaks around  $(\pi, \pi)$ , the  $q$ -width at a given  $\omega$ , the Boltzmann constant and an overall scale factor, respectively.  $\kappa_\omega$  is assumed to be isotropic in the  $\text{CuO}_2$  plane.

The imaginary part of the  $q$ -integrated dynamical susceptibility averaged over the Brillouin zone is defined as:

$$\chi''(\omega)/\omega = \int \chi''(q, \omega) dq / (\omega \cdot \int dq) \quad (3)$$

Note that in this case, the  $q$ -integration is carried out for the four incommensurate peaks around  $(\pi, \pi)$  over the Brillouin zone.

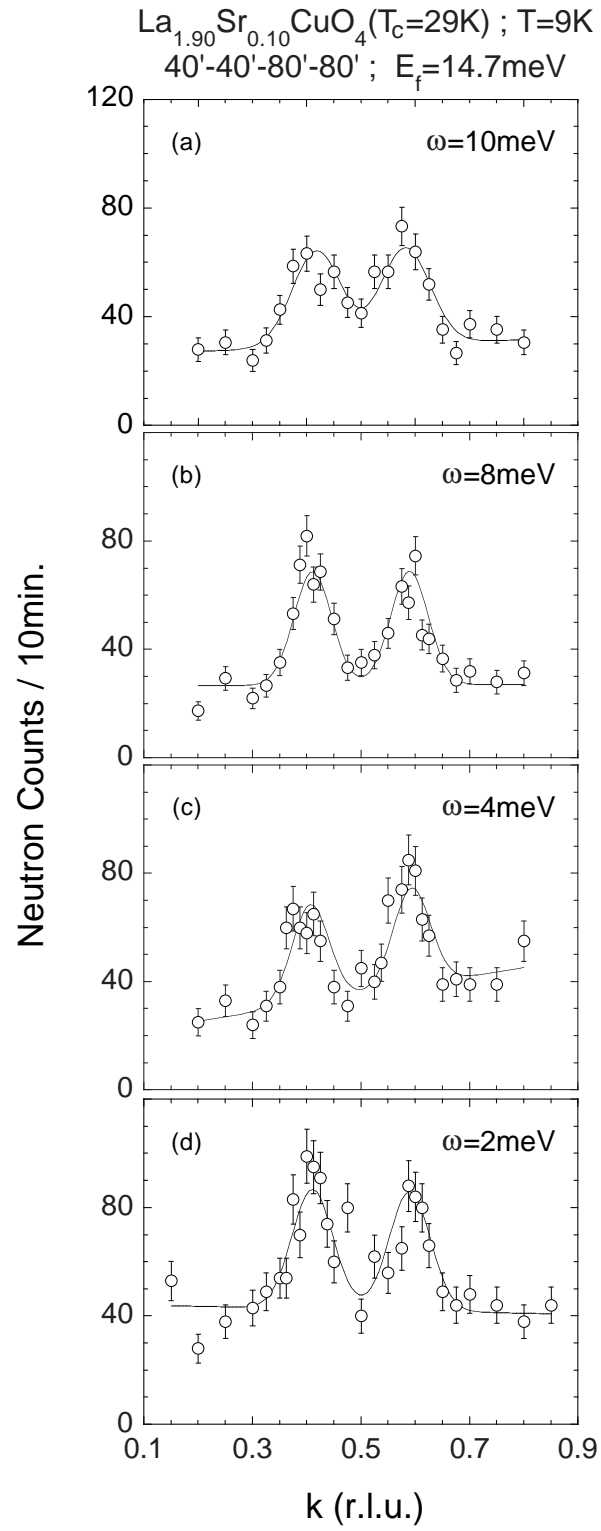


FIG. 2. Q-spectra at different energies obtained by the same scan as in Fig. 1 for  $x=0.10$  below  $T_c$

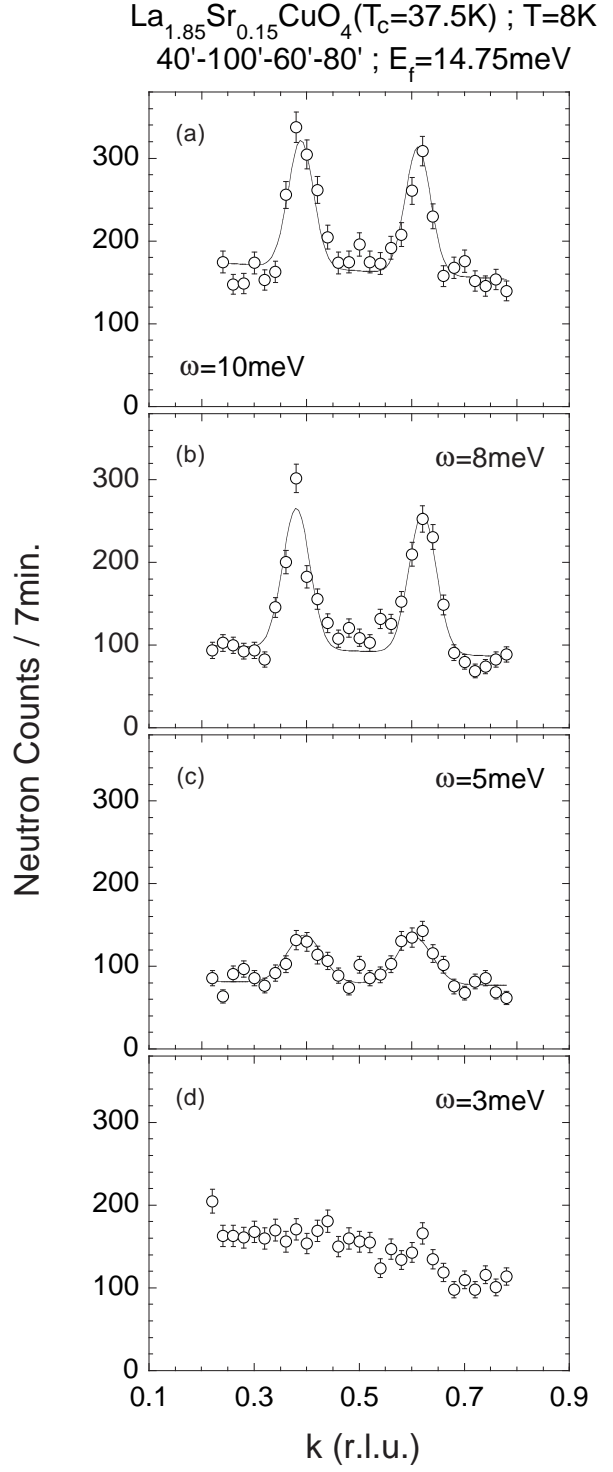


FIG. 3. Q-spectra at different energies obtained by the same scan as in Fig. 1 for  $x=0.15$  below  $T_c$ .

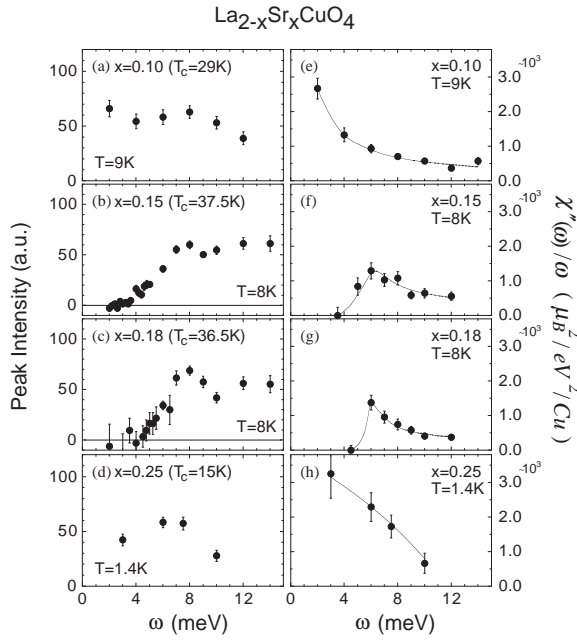


FIG. 4. Energy dependence of the intensity at the incommensurate peak position below  $T_c$  for  $x=0.10$ (a), 0.15(b), 0.18(c) and 0.25(d). Panels (e) - (h) depict the energy dependence of  $\chi''(\omega)/\omega$  calculated by using the fitted results of the q-spectra.

In Fig. 4, we show the energy-dependence of the peak intensities at the incommensurate positions for  $x = 0.10, 0.15, 0.18$  and  $0.25$  together with the resolution-corrected  $\chi''(\omega)/\omega$ , which is obtained by fitting the q-spectrum and integrating over  $q$  for the four incommensurate peaks around  $(\pi, \pi)$ . The absolute value of  $\chi''(\omega)/\omega$  for each sample was calculated by using phonon intensities for the same sample as described in the Appendix. We present  $\chi''(\omega)/\omega$  instead of  $\chi''(\omega)$  to reveal any gap structure in the spectrum because the latter quantity may go to zero as the energy approaches zero even if there is no gap. Fig. 4 again exhibits two types of energy dependencies for the incommensurate peaks for the four samples. There exists a well-defined energy gap for  $x = 0.15$  and  $0.18$ , accompanied by an enhancement of  $\chi''(\omega)/\omega$  around  $6$  meV to  $7$  meV while no gap-like structure is seen for  $x = 0.10$  and  $0.25$ .

The energy dependence of the resolution-corrected

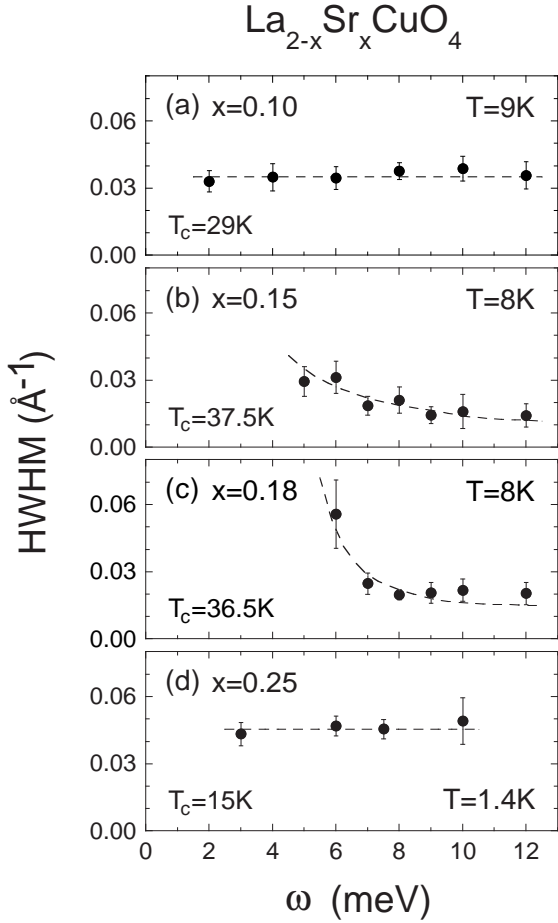


FIG. 5. Energy dependence of the q-width of an incommensurate peak below  $T_c$  with the instrumental resolution deconvolved. The q-width in the low energy region for  $x=0.15$  and  $0.18$  cannot be obtained due to the opening of the energy gap below  $T_c$ .

q-width of the incommensurate peak below  $T_c$  is shown in Fig. 5. We only show the data above  $5$  and  $6$  meV for  $x = 0.15$  and  $0.18$ , respectively because of the energy gap. We note that the q-width has a rather different  $\omega$  dependence depending on whether or not there is a gap. For the gapped samples, above the gap energy the q-width is small and it increases with decreasing energy as the gap energy is approached. Furthermore, as will be shown later in Fig. 8, for  $T \sim T_c$  the q-width appears to exhibit a peak for excitation energies near the gap energy. On the other hand, for the gapless samples the q-width

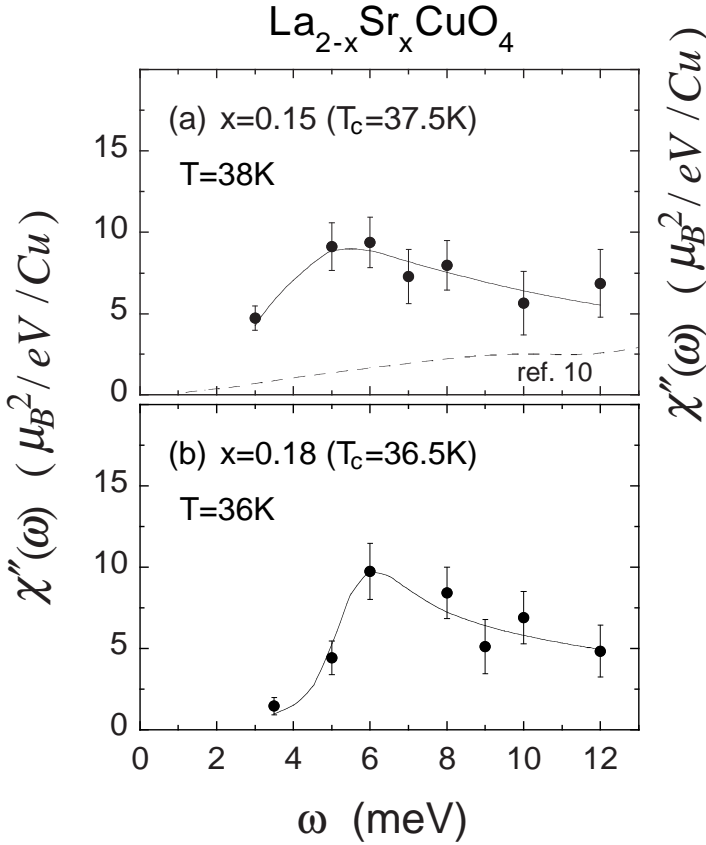


FIG. 6. Energy dependence of  $\chi''(\omega)$  for  $x=0.15$ (a) and  $0.18$ (b) around  $T_c$ . The solid lines are the results of a least squares fit using the gap-function, Eq. (4), convoluted with the instrumental resolution function. The broken line in the upper panel is a smoothed interpolation of the data for  $x=0.14$  reported in ref. [10].

is constant with energy at least up to 12 meV.

Next, we show  $\chi''(\omega)$  for temperatures  $T \sim T_c$  for  $\text{La}_{2-x}\text{Sr}_x\text{CuO}_4$  crystals with  $x=0.15$  and  $0.18$  in Fig. 6. Although the peak in the intensity appears at slightly lower energies compared to the data below  $T_c$ , a gap-like structure and an enhancement in  $\chi''(\omega)$  still remains. In the upper panel of Fig. 6, we show using a dashed line the data obtained by Hayden *et al.* for the same system with  $x=0.14$  [10]. No peak in  $\chi''(\omega)$  is observed in their data. As shown in Fig. 7, for the gapless sample of  $\text{La}_{2-x}\text{Sr}_x\text{CuO}_4$  with  $x=0.10$ , both the energy and temperature variation

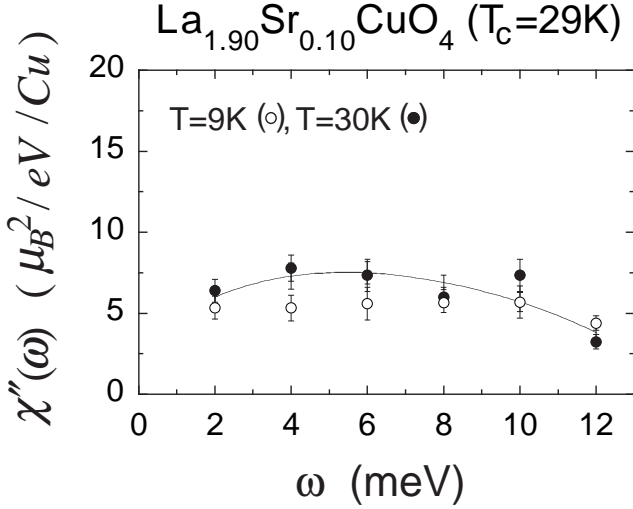


FIG. 7. Energy spectra of  $\chi''(\omega)$  for  $x=0.10$  below and around  $T_c$ .

of  $\chi''(\omega)$  is weak, although we see a slight suppression of  $\chi''(\omega)$  around 4 to 6 meV at  $T=9\text{K}$ .

In Fig. 8 we show the energy variation of the q-width of the incommensurate peak for  $T \sim T_c$  for  $x=0.15$  and in the inset for  $x=0.18$ . In the figure, we have plotted results from several different crystals. We observe a peak in the q-width at around the same energy as that at which the enhancement of  $\chi''(\omega)$  is observed. In contrast, the energy variation of the q-width for the sample with  $x=0.14$  of Aeppli *et al.* [11] shows a linear energy dependence. It should be noted that the peak width for energies of order 8 to 10 meV is substantially narrower below  $T_c$  than that at  $T_c$  for the gapped samples, particularly for  $x=0.18$ .

#### IV. Discussion

The present study has revealed two types of energy spectra for the spin fluctuations in Sr-doped superconducting  $\text{La}_2\text{CuO}_4$ . For  $x=0.15$  and  $0.18$ , a well-defined energy gap appears below  $T_c$ , whereas for the underdoped sample,  $x=0.10$ , and highly overdoped sample,  $x=0.25$ , no gap is observed even

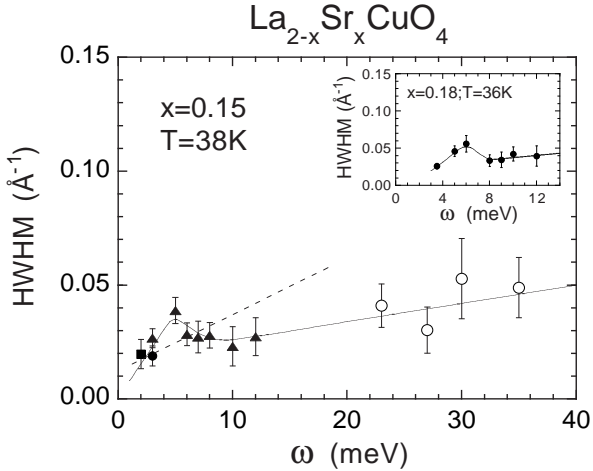


FIG. 8. Energy dependence of the q-width of an incommensurate peak around  $T_c$  deconvoluted with the instrumental resolution for  $x=0.15$  and  $0.18$ (inset). The broken line is drawn to represent the data for  $x=0.14$  reported in ref. [11].

though they exhibit bulk superconductivity with  $T_c=29K$  for  $x=0.10$  and  $T_c=15K$  for  $x=0.25$ .

In order to discuss the results shown in Figure 4 quantitatively, we introduce a phenomenological dynamical spin susceptibility of the form:

$$\frac{\chi''(\omega)/\omega}{\left(B\frac{\gamma}{\gamma^2 + \omega^2}\right) \cdot \text{Re} \left(\frac{\omega - i\Gamma}{\sqrt{(\omega - i\Gamma)^2 - \Delta^2}}\right)} = \quad (4)$$

This corresponds to Lorentzian spin fluctuations in the normal state multiplied by a gap-function in the superconducting state. The gap function includes the gap-energy  $\Delta$  together with a broadening  $\Gamma$ ;  $\gamma$  is the inverse of lifetime of the spin fluctuations. The parameters  $B$ ,  $\Delta$  and  $\Gamma$  are assumed to be constant in the q-region of the incommensurate peaks. It should be noted that in Eq. (4),  $\chi''(\omega)/\omega$  is a simple Lorentzian in energy for  $\Delta = 0$ . On the other hand, in the superconducting state, Eq. (4) describes the gap-structure with a non-zero value of  $\Delta$ . As required, the above dynamical spin susceptibility satisfies detailed balance for the dynamical structure factor  $S(q, \omega)$ .

The observed energy spectra were fitted using Eq. (4) convoluted with the instrumental energy resolution. The value of  $\Delta$  so-obtained is  $6 \pm 0.3$  meV for both  $x=0.15$  and  $0.18$  while  $\Gamma = 0.6 \pm 0.3$  meV for  $x=0.15$  and  $= 0 \pm 0.2$  meV for  $x=0.18$ . Quite recently, Lake *et al.* reported a similar value for the energy-gap for a sample of  $La_{2-x}Sr_xCuO_4$  with  $x=0.16$  [25]. We note that  $\Delta$  is significantly larger than the value previously quoted by our collaboration which was around 3.5 meV for  $x=0.15$  [7]. However, this latter value for the energy-gap was simply the energy below which the magnetic intensity disappeared entirely below  $T_c$ . This energy is naturally less than our fitted value simply due to the non-zero broadening of the gap-structure for  $x=0.15$  together with the effects of instrumental resolution. We note that for samples with  $x=0.14$  and  $0.16$ , Lake *et al.* [25] find  $\Gamma = 1.2$  meV and  $0.1$  meV respectively albeit using a somewhat different functional form than Eq. (4). Thus,  $\Gamma$  decreases smoothly with increasing  $x$  reaching 0 within the errors for  $x=0.18$  while the gap energy  $\Delta$  appears to be independent of  $x$  for  $x$  between 0.14 and 0.18.

In Ref. 6 the gap-energy,  $\Delta_m^{inc}$  of the spin fluctuations at the incommensurate peak position was converted into the value at  $(\pi, 0)$  by assuming a  $d(x^2 - y^2)$ -type q-dependence. The previous value  $\Delta_m^{inc} \sim 3.5$  meV implied a full gap of  $\sim 10$  meV which is consistent with the full superconducting gap of  $\sim 8$  meV inferred from photoemission spectroscopy [26]. However, the new value of  $\Delta_m^{inc}$  determined here implies a full gap of  $\sim 18$  meV which corresponds to  $\Delta = 5.6kT_c$  which seems too high compared with the BCS weak coupling value of  $1.77 kT_c$ . This fact, therefore, suggests that  $\Delta_m^{inc}$  may not be simply related to the superconducting gap. It is possible that  $\Delta_m^{inc}$  instead relates to the so-called pseudo-gap or the larger energy gaps reported by photoemission

and tunneling spectroscopies.

The gapped samples exhibit an anomalous broadening in the  $q$ -width of the incommensurate peaks for energies around the gap value of  $\Delta_m^{inc}$ . Qualitatively, we can interpret the peak-broadening as arising from the energy independent dispersion surface of the quasiparticle excitations around the energy-gap. In other words, if the magnetic scattering occurs through interband excitations of quasiparticles, the momentum change can be widely distributed for excitation energies close to the gap. As shown in Fig. 8, a broadening in  $q$  of the peak width for energies of order  $\Delta$  is observed at  $T_c$  which again indicates the robustness of the gap structure of  $\chi''(\omega)$  for the gapped samples.

We discuss next the possible reasons for the absence of an energy-gap in the gapless samples with  $x=0.10$  and  $x=0.25$ . At present, it is widely speculated without any direct experimental evidence that the disorder introduced by dopant substitution at the La-sites degrades the lifetime of the quasiparticles and smears out the gap structure. However, this is contradicted by the fact that no gap is observed in either stage-6 or stage-4  $\text{La}_2\text{CuO}_{4+y}$  in spite of the fact that structural disorder is minimal in these systems [27,28]. Further, neutron scattering experiments on the Y1-2-3 system reveal the robustness of the magnetic energy-gap against Zn-impurities [29,30]. In the Zn-doped Y1-2-3 system, although low energy spin fluctuations appear at low temperatures, the gap-like or pseudo-gap structure appears at higher temperatures.

For the  $x=0.10$  sample, the low energy spin excitations are simply explained as originating from the spin wave excitations concomitant with the elastic magnetic order which occurs in the superconducting state. Such order is observed for all  $x$  between 0.02 and 0.135 in  $\text{La}_2\text{CuO}_4$ . However, a different ex-

planation is required for the highly overdoped gapless sample,  $x=0.25$ , because in that case there is no evidence for magnetic order coexisting with the superconductivity. Here, we simply point out that there is a dramatic degradation of the spacial coherence of the spin correlations in the overdoped region particularly near the upper critical doping value for the superconductivity as pointed out by Yamada et al. [15]. In this doping region, the spatial coherence length for the low energy spin fluctuations becomes comparable to or shorter than the superconducting coherence length. Therefore, the energy gap in this region is probably vitiated by the degradation of the lifetime of quasiparticles due to the short ranged spin fluctuations.

## V. Summary

We have studied the energy dependence of the spin fluctuations for superconducting  $\text{La}_{2-x}\text{Sr}_x\text{CuO}_4$  ( $x=0.10, 0.15, 0.18, 0.25$ ) using neutron inelastic scattering. Below  $T_c$  a well-defined energy gap in the incommensurate spin fluctuations is observed in the superconducting state of the optimally doped ( $x = 0.15$ ) and slightly over doped ( $x = 0.18$ ) samples. An enhancement in  $\chi''(\omega)$  caused by the peak-broadening is also observed at  $\sim 6$  meV which remains even at  $T_c$ . For the underdoped sample with  $x = 0.10$  and the highly overdoped sample with  $x = 0.25$ , no clear gap is observed even though these samples show bulk superconductivity.

## Acknowledgements

The authors acknowledge K. Nemoto and M. Onodera for their technical assistance at JAERI and Tohoku University. We wish to thank H. Fukuyama, T. Tanamoto, H. Kohno, S. Hosoya, K. Hirota and H. Kimura for valuable discussions. We also thank S. Wakimoto for his help in crystal growth of  $x=0.15$

samples. The present work was supported in part by a Grant-In-Aid for Scientific Research from the Ministry of Education, Science, Culture and Sports of Japan and a Grant for the Promotion of Science from the Science and Technology Agency of CREST. Work at Brookhaven National Laboratory was carried out under contract No. DE-AC02-98CH10886, Division of Material Science, U. S. Department of Energy. The research at Massachusetts Institute of Technology was supported by the National Science Foundation under Grant No. DMR97-04532 and the MRSEC Program of the National Science Foundation under Award No. DMR98-08941.

## Appendix

We have converted the observed magnetic intensity into the absolute value of  $\chi''(\omega)$  by comparing with the intensity of phonon scattering. The phonon intensity is given by

$$I_\nu = \alpha \cdot \left( \frac{d\sigma}{d\Omega} \right) \quad (5)$$

where  $\alpha$  is the detector efficiency and  $I_\nu$  is the energy-integrated phonon intensity measured by constant- $Q$  scans. The energy integrated phonon scattering cross section is given by:

$$\left( \frac{d\sigma}{d\Omega} \right) = C \frac{|F|^2}{M} \frac{|Q|^2 \cos^2 \beta \cdot N}{\hbar \omega} e^{-2W} \langle n+1 \rangle \quad (6)$$

where  $C=2.09$  barns,  $F$  is the nuclear structure factor,  $M$  is the total atomic mass in a unit cell,  $\beta$  is the angle between  $Q$  and the phonon polarization direction,  $N$  is the number of unit cells,  $e^{-2W}$  is the Debye-Waller factor and  $\langle n+1 \rangle$  is the population factor. We have measured the integrated intensity of the acoustic phonons by constant- $Q$  scans at  $(2, -0.13, 0)$  for  $x = 0.10$  and  $(2, -0.17, 0)$  for  $x = 0.15, 0.18$ , and  $0.25$ . The magnetic scattering intensity is measured by constant- $\omega$  scans. To scale the magnetic scattering intensity with the phonon intensity measured in a different scan mode,  $I_\nu$  is divided by the sound velocity. The absolute value of  $\chi''(q, \omega)$  is estimated using the following magnetic cross section per formula unit for a Heisenberg system without Néel ordering:

$$\left( \frac{d^2\sigma}{d\Omega d\omega} \right) = r_0^2 \frac{k_f}{k_i} \left[ \frac{g}{2} f(Q) e^{-W} \right]^2 \sum_{\alpha} (1 - \hat{k}_{\alpha}^2) S^{\alpha}(Q, \omega) \quad (7)$$

$$S^{\alpha}(Q, \omega) = \frac{1}{\pi} \frac{1}{g^2 \mu_B^2} \langle n+1 \rangle \text{Im} \chi^{\alpha}(Q, \omega) \quad (8)$$

Here  $r_0^2 = 0.291$  barns,  $f(Q)$  is magnetic form factor and  $\hat{k} = Q/|Q|$ .

<sup>1</sup>For a review, see M. A. Kastner, R. J. Birgeneau, G. Shirane and Y. Endoh, Rev. Mod. Phys. **70**, 897 (1998).

<sup>2</sup>H. Yasuoka, T. Imai and T. Shimizu, Springer Series in Solid State Science 89, Strong Correlation and Superconductivity, ed. H. Fukuyama, S. Maekawa and A. P. Malozemoff (Springer-Verlag, New York, 1989)

<sup>3</sup>J. Rossat-Mignod, L. P. Regnault, C. Vettier, P. Bourges, P. Burlet, J. Bossy, J. Y. Henry and G. Lapertot, Physica C **185-189**, 86 (1991)

<sup>4</sup>T. E. Mason, G. Aeppli and H. A. Mook, Phys. Rev. Lett. **68**, 1414 (1992)

<sup>5</sup>J. M. Tranquada, P. M. Gehring, G. Shirane, S. Shamoto and M. Sato, Phys. Rev. B. **46**, 5561 (1992)

<sup>6</sup>M. Matsuda, K. Yamada, Y. Endoh, T. R. Thurston, G. Shirane, R. J. Birgeneau, M. A. Kastner, I. Tanaka and H. Kojima, Phys. Rev. B **49**, 6958 (1994)

<sup>7</sup>K. Yamada, S. Wakimoto, G. Shirane, C. H. Lee, M. A. Kastner, S. Hosoya, M. Greven, Y. Endoh, and R. J. Birgeneau, Phys. Rev. Lett. **75**, 1626 (1995)

<sup>8</sup>K. Yamada, Y. Endoh, C. H. Lee, S. Wakimoto, M. Arai, K. Ubukata, M. Fujita, S. Hosoya and S. M. Bennington, J. Phys. Soc. Jpn. **64**, 2742 (1995)

<sup>9</sup>M. Arai, T. Arakawa, M. Fujita, S. Wakimoto, K. Yamada, Y. Endoh, G. Aeppli, T. E. Mason and S. M. Hayden, Czech. J. Phys. **46**, Suppl. S2, 1147 (1996)

<sup>10</sup>S. M. Hayden, G. Aeppli, H. A. Mook, T. G. Perring, T. E. Mason, S.-W. Cheong and Z. Fisk, Phys. Rev. Lett. **76**, 1344 (1996)

<sup>11</sup>G. Aeppli, T. E. Mason, S. M. Hayden, H. A. Mook, J. Kulda, Science **278**, 1432 (1997)

<sup>12</sup>Y. Itoh, M. Matsumura and H. Yamagata, J. Phys. Soc. Jpn. **66**, 3383 (1997)

<sup>13</sup>S. Hosoya, C. H. Lee, S. Wakimoto, K. Yamada and Y. Endoh, Physica C **235-240**, 547, (1994)

<sup>14</sup>C. H. Lee, N. Kaneko, S. Hosoya, K. Kurahashi, S. Wakimoto, K. Yamada and Y. Endoh, Supercond. Sci. Technol. **11**, 891, (1998)

<sup>15</sup>K. Yamada, C. H. Lee, K. Kurahashi, J. Wada, S. Wakimoto, S. Ueki, H. Kimura, Y. Endoh, S. Hosoya, G. Shirane, R. J. Birgeneau, M. Greven, M. A. Kastner and Y. J. Kim, Phys. Rev. B **57**, 6165 (1998)

<sup>16</sup>R. M. Fleming, B. Batlogg, R. J. Cava and E. A. Rietman, Phys. Rev. B **35**, 7191 (1987)

<sup>17</sup>H. Takagi, R. J. Cava, M. Marezio, B. Batlogg, J. J. Krajewski, W. F. Peck, Jr., P. Bordet and D. E. Cox, Phys. Rev. Lett. **68**, 3777 (1992)

<sup>18</sup>T. Nagano, Y. Tomioka, Y. Nakayama, K. Kishio and K. Kitazawa, Phys. Rev. B **48**, 9689 (1993)

<sup>19</sup>C. H. Lee, K. Yamada, M. Arai, S. Wakimoto, S. Hosoya, Y. Endoh, Physica C **257**, 264 (1996)

<sup>20</sup>K. Kurahashi, S. Wakimoto, C. H. Lee, K. Yamada and S. Hosoya, J. Phys. Soc. Jpn. **65**, 3994 (1996)

<sup>21</sup>H. Takagi, T. Ido, S. Ishibashi, M. Uota, S. Uchida and Y. Tokura, Phys. Rev. B **40**, 2254 (1989)

<sup>22</sup>R. Yoshizaki, N. Kuroda, S. Nakamura and N. Ishikawa, Physica C **199**, 143 (1992)

<sup>23</sup>T. Nakano, M. Oda, C. Manabe, N. Momono, Y. Miura, and M. Ido, Phys. Rev. B **49**, 16000 (1994)

<sup>24</sup>D. C. Johnston, Phys. Rev. Lett. **62**, 957 (1989)

<sup>25</sup>B. Lake, G. Aeppli, T. E. Mason, A. Schröder, D.F. McMorrow, K. Lefmann, M. Isshiki, M. Nohara, H. Takagi and S. M. Hayden, Nature **400**, 43 (1999).

<sup>26</sup>T. Sato, T. Yokoya, Y. Naitoh, T. Takahashi, K. Yamada and Y. Endoh, Phys. Rev. Lett. **83**, 2254 (1999).

<sup>27</sup>B. O. Wells, Y. S. Lee, M. A. Kastner, R. H. Christianson, R. J. Birgeneau, K. Yamada, Y. Endoh and G. Shirane, Science **277**, 1067 (1997).

<sup>28</sup>Y. S. Lee, R. J. Birgeneau, M. A. Kastner, Y. Endoh, S. Wakimoto, K. Yamada, R. W. Erwin, S. -H. Lee and G. Shirane, Phys. Rev. B **60**, 3643 (1999).

<sup>29</sup>H. Harashina, S. Shamoto, T. Kiyokura, M. Sato, K. Kakurai and G. Shirane, J. Phys. Soc. Jpn. **62**, 4009 (1993).

<sup>30</sup>P. Bourges, Y. Sidis, B. Hennion, R. Villeneuve, J. F. Marucco and G. Collin, Czech. J. Phys. **46**, Suppl. S2, 1155 (1996).